Rare Metal Materials and Engineering
Volume 45, Issue 12, December 2016
Online English edition of the Chinese language journal

Available online at www.sciencedirect.com
ScienceDirect

Cite this article as: Rare Metal Materials and Engineering, 2016, 45(12): 3037-3042.

ARTICLE

Effect of Glass Additions on $Ca_{0.8}Sr_{0.2}TiO_3$ Ceramics as Dielectrics for a Cylindrical Dielectric Barrier Discharge Reactor in CO_2 Plasma

Song Xiaozhen, Zhang Yong, Qu Fuyang, Wang Xiangrong

Beijing Key Laboratory of Fine Ceramics, State Key Laboratory of New Ceramics and Fine Processing, Tsinghua University, Beijing 100084, China

Abstract: The $Ca_{0.8}Sr_{0.2}TiO_3$ ceramics with different amounts of glass addition were prepared by liquid phase sintering and used as dielectric barriers in a cylindrical dielectric barrier discharge reactor to decompose carbon dioxide at atmospheric pressure. Results show that the surface resistivity increases with increasing glass content. While the dielectric constant does not change obviously with the increase of the glass content in the investigated temperature range. The scanning electron microscope observations indicate that both the grain size and the thickness of intergranular glassy phases increase with the increase of the glass content. More importantly, the conversion rate and conversion efficiency of carbon dioxide improve with the increase of glass content in the ceramics. Furthermore, a combined discharge analysis and dielectric characterization are modeled with a Malter effect approach. From this model, it is possible to interpret the relationship between the conversion characteristics and the glass content in the ceramic samples.

Key words: dielectric barrier discharge; conversion rate; conversion efficiency; carbon dioxide

The mitigation of greenhouse gases has aroused tremendous interests in recent years because there has been growing acceptance of evidence of a link between global climate change and greenhouse gas content in the atmosphere. Carbon dioxide, which contributes about 55% among all the greenhouse gases, is emitted annually from the combustion of fossil fuel. In order to limit the environmental effects of carbon dioxide, three main strategies including limitation of the emissions, capture, and degradation can be explored. The degradation of carbon dioxide into valuable chemicals through plasma based technologies could provide a solution to the substantial progress in carbon dioxide mitigation if the electrical energy is from a low carbon emitting (renewable or nuclear) power plant.

Recently, a physical route called dielectric barrier discharge (DBD) which has been widely used in many aspects, including surface modification[1], pollution control[2], and ozone generation[3], is utilized to decompose carbon dioxide. The characteristic feature of the DBD is the dielectric barrier placed between or attached to electrodes[4]. In fact, the DBD can be highly influenced by the properties of dielectric material, which not only limits the amount of charges but also distributes the microdischarges over the entire electrode/barrier area [5].

This has triggered a research effort in materials development with good properties. The dielectric properties of the barrier material as well as their effects on the discharge process have been examined by several groups[6-8]. The low surface resistivity which could enhance the fast surface charge spreading, has been reported to contribute to the discharge uniformity in the discharge gap[6]. Also, charges trapped into the shallow traps with energy level lower than 1 eV on the dielectric surface have some influence on the uniform discharge[7]. Moreover, high dielectric constant of the dielectric barrier could improve the average plasma

Received date: December 28, 2015
Foundation item: International Science & Technology Cooperation Program of China (2012DFR50560)
Corresponding author: Zhang Yong, Ph. D., Professor, Institute of Nuclear and New Energy Technology, Tsinghua University, Beijing 100084, P. R. China, Tel: 0086-10-80194055, E-mail: yzhang@tsinghua.edu.cn

power obviously[8] and produce much more charges in the discharge gap[9].

Our early work[10] characterizes the dominant role of the surface charge trapped in grain boundaries during the discharge. In the present paper, we employed varying amounts of glass added dielectric ceramics as dielectric barriers to assess the effect of glass contents on the decomposition behavior of carbon dioxide. The discharge power, conversion rate and conversion efficiency were compared to these dielectric barriers. More importantly, a mechanistic model for observed phenomenon was proposed to explain the relationship between the conversion characteristics and the glass content in the ceramic samples.

1 Experiment

Bulk $Ca_{0.8}Sr_{0.2}TiO_3$ (CST) ceramic samples were prepared by conventional solid state reaction using analytical reagent grade powders of $CaCO_3$, $SrCO_3$ and TiO_2. They were stoichiometrically mixed by ball milling for 6 h using ethanol as medium with ZrO_2 balls in polyethylene jars. Then, the mixture was dried at 90 ℃ and calcined at 1130 ℃ for 2 h. The glass BaO-B_2O_3-SiO_2-CaO-SrO-Bi_2O_3-Al_2O_3-ZrO_2 (BBS) was prepared from reagent grade powders of 47.25 $BaCO_3$, 22.59 H_3BO_3, 8.34 SiO_2, 3.42 $CaCO_3$, 5.05 $SrCO_3$, 9.56 Bi_2O_3, 2.09 Al_2O_3, and 1.70 ZrO_2 (wt%). Well mixed powder containing appropriate quantities of the above chemicals were melted in a platinum crucible at 1200 ℃ for 1 h. Then, the molten material was rapidly poured into a container filled with distilled water. Subsequent particle size reduction of the glass frit was undertaken by ball milling for 6 h.

The calcined $Ca_{0.8}Sr_{0.2}TiO_3$ powder was mixed with the glass in terms of the composition (100–x) $Ca_{0.8}Sr_{0.2}TiO_3$ + x glass (x = 0.5, 1.0 and 5.0 wt%) by ball milling for 6 h with ZrO_2 balls. After dried, the mixture was granulated with polyvinyl alcohol (PVA) binder and uniaxially pressed into pellets 30 mm in diameter and 1.5 mm in thickness at the pressure of 40 MPa. The pellets were sintered at 1180 ℃ for 3 h with a heating rate 3 ℃/min. For dielectric measurements, the specimens were polished and then heat-treated at 550 ℃ for 0.3 h after pasted with silver paste.

The microstructure observation and analysis of the fracture surfaces of the ceramic specimens were performed with a scanning electron microscope (SEM: FEI Qunanta 200 FEG). The temperature dependences of dielectric constant were measured at 100 kHz by means of a LCR meter (HP 4284A, Palo Alto, CA, USA) from −60 ℃ to 180 ℃. Surface temperature was measured through an infrared radiation thermometer (MSPro, Optris, Germany). Measurements of the surface resistance were carried out by a Megger (ZC36, Shanghai Sixth Electric meter factory Co. Ltd., China). Then the surface resistance was converted to the surface resistivity by

$$\rho_s = R_s \frac{2\pi}{\ln(\frac{d_1}{d_2})} \quad (1)$$

where ρ_s is the surface resistivity, R_s is the surface resistance, d_1, d_2 are the diameters of low voltage electrode and high voltage electrode, respectively.

The experimental setup for the CO_2 decomposition is shown in Fig.1. The DBD plasma chamber, which was made from silica glass, was used for the decomposition of CO_2. The gas mixture (CO_2:N_2 = 10:90) was fed into two circular parallel-plate electrodes (29.6 mm in diameter) made from aluminum at a flow rate 300 mL/min, where the ground electrode was covered with a dielectric barrier. The gap space between the dielectric barrier and the counter-electrode was 0.5 mm and the experiment was carried out at atmospheric pressure by a conventional flow system. The CO_2 content was analyzed by a gas chromatograph (GC Agilent 6820). The conversion rate (C_R) was calculated by Eq.(2):

$$C_R = \frac{n(CO_2)_{converted}}{n(CO_2)_{introduced}} \times 100\% \quad (2)$$

where $n(CO_2)_{converted}$ means the moles of CO_2 which has been converted during the decomposition, while $n(CO_2)_{introduced}$ means the moles of CO_2 which has been introduced into the chamber during discharge.

A sinusoidal voltage applied to the electrodes was amplified to 5 kV by an ac amplifier to bring about intense plasma reaction. The output current was measured from the voltage drop across a resistor (R = 50 Ω) in series with the ground electrode. The output voltage (U) was measured with the voltage divider of the resistors R_1 and R_2 (R_1:R_2 = 1:1000) by the digital oscilloscope (DPO 3014, Tektronix). The discharge power (P) was calculated according to the V-Q Lissajous method, as shown in Eq.(3). The charge Q = uC_0 is determined by measuring the voltage across the capacitor (C_0 = 0.47 μF) which was connected to the ground electrode. The voltage (u) across the capacitor and the frequency (f) were monitored and recorded by the digital oscilloscope. The integral had to be extended over one

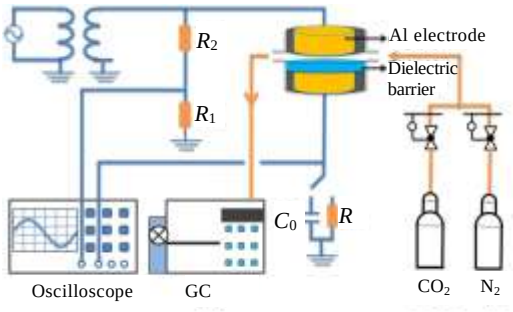

Fig.1 Schematic diagram of experimental apparatus

period T of the applied voltage. The discharge power (P) and the conversion efficiency (C_E) were calculated by the following equations:

$$P = f\int_0^T U\mathrm{d}Q = f\int_0^T U\mathrm{d}(C_0 u) = fC_0\int_0^T U\mathrm{d}u \quad (3)$$

$$C_E = \frac{C_R}{P}\times 100\% \quad (4)$$

2 Results and Discussion

2.1 Dielectric properties of the barriers

The CST ceramics with various BBS glass additions were sintered at 1180 ℃. The ceramic samples currently under investigation have been prepared using equivalent processing to the samples considered in Ref.[10] except that the added glass composition was different. The surface resistance has been measured on ceramic samples with various glass contents. Fig.2 depicts the surface resistivity as a function of glass content. We find that the surface resistivity increases with the increase of glass content.

Fig.3 shows the temperature dependence of the dielectric constant for the CST ceramics with different BBS glass additions. Obviously, the dielectric constant is decreased with the increase of temperature in the measuring temperature range. This decrease arises from the paraelectric phase in which the CST ceramics locate.

2.2 Microstructural analysis of the dielectric barriers

The microstructure of the ceramic samples with different glass additions was evaluated through the SEM observation. Fig.4 shows SEM micrographs of the ceramic samples with different glass contents. As shown in Fig.4, the glass phase can be seen at grain boundaries in the glass added CST ceramics. During the process of sintering the added glass phase might produce a liquid phase with a lower melting point. Thus the density of the ceramic samples increases. The observations indicate that both the grain size and the thickness of intergranular glass phases increase with the increase of the glass content.

2.3 Discharge properties

The DBD experiment was carried out to decompose carbon dioxide in the plasma chamber. A typical image of the surface of the dielectric barrier after DBD experiment is illustrated in Fig.5. As shown, carbon deposition is observed on the surface of the ceramic sample, clearly showing a decomposition of carbon dioxide. The gas which had been subjected to the DBD experiment was analyzed by gas chromatography. The peak identities are shown in Fig.6.

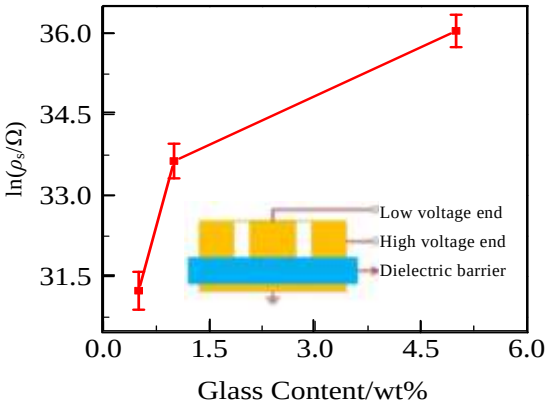

Fig.2 Surface resistivity versus glass content for the CST ceramics (the inset shows the configuration of the three electrode)

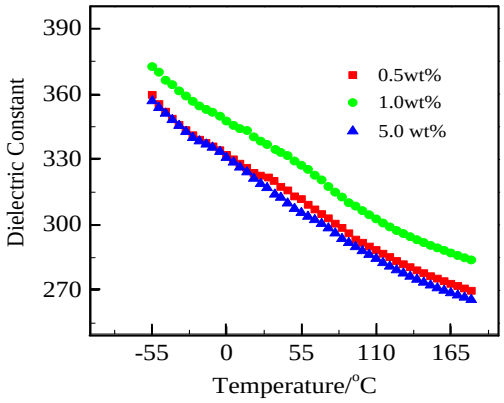

Fig.3 Temperature dependence of dielectric constant at 100 kHz for the CST ceramics with different BBS glass contents

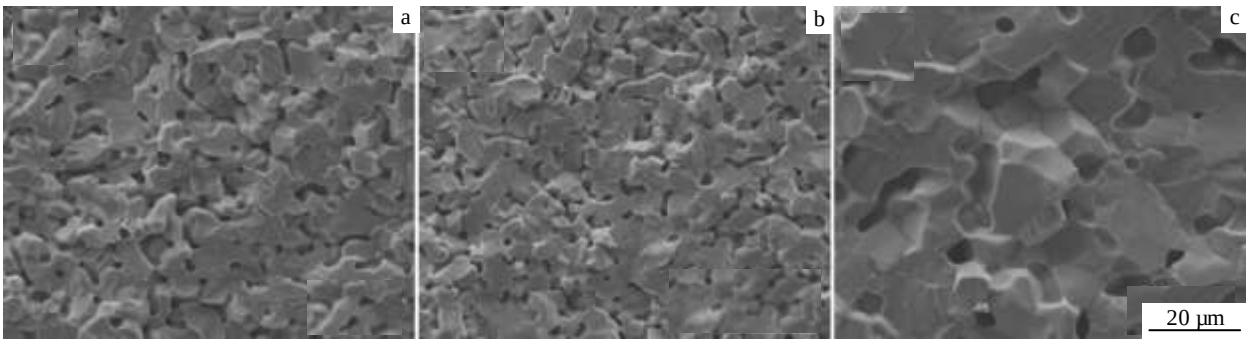

Fig.4 SEM micrographs of the CST ceramics with different BBS glass amounts: (a) 0.5 wt%, (b) 1.0 wt%, and (a) 5.0 wt%

Fig.5 Photograph of the surface of the CST ceramic with 1.0 wt% glass addition after DBD experiment

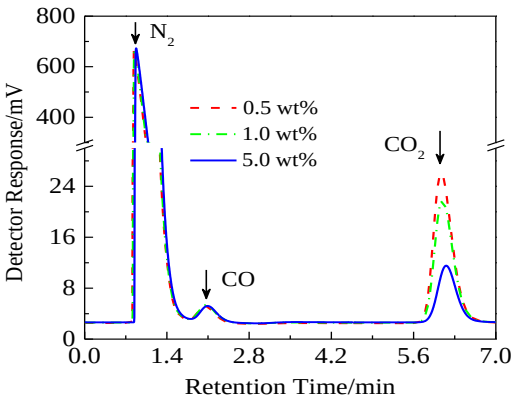

Fig.6 Chromatogram of the gases after DBD experiment for the CST ceramics with different BBS glass addition

As a result, one can believe that the decomposition of carbon dioxide proceeds as follows:

$$CO_2+e \rightarrow CO+1/2O_2+e \quad (5)$$

$$CO+e \rightarrow C+1/2O_2+e \quad (6)$$

Further, there exists a decreasing tendency with increasing glass content, which suggests that the conversion rate of car bon dioxide increases gradually.

Fig.7 demonstrates the current and voltage waveforms during the discharge at ac frequency of 6.5 kHz when the gap space equals to 0.5 mm. Basically, there is only one current pulse per half cycle, which characterizes the stable homogenous discharge as is reported by previous investigations[11].

A characteristic curve of the charge versus the voltage in the presence of discharge for the CST ceramics with 1.0 wt% glass addition is shown in Fig.7, which is used to calculate the discharge power. The discharge power was confined to the range of 11.20~11.60 W with slightly lower power occurring in the samples added with 1.0 wt% glass addition. The ceramic samples added with 0.5 wt% and 1.0 wt% glass show only small differences in both C_R and C_E of CO_2. It should be mentioned that the two parameters increase with the increase of the BBS glass content.

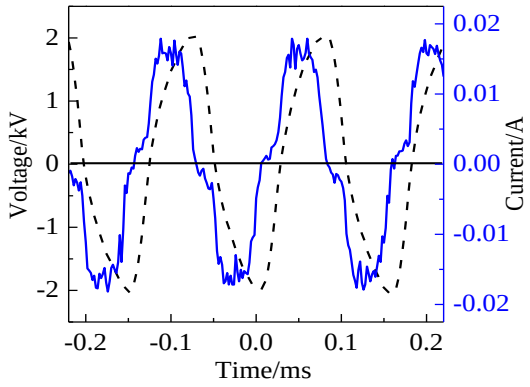

Fig.7 Current and voltage waveforms for the CST ceramics with 1.0wt% BBS glass addition during the plasma reaction

The general CO_2 decomposition characteristics of the CST ceramics as a function of glass content are summarized in Table 1.

2.4 Mechanistic model for observed phenomenon

The fundamentals of dielectric barrier discharge, in conjunction with the literature on the dielectric ceramics, provide a consistent explanation for the CO_2 decomposition behavior observed in the DBD experiment. We begin with two interpretations related to the changes of C_R and C_E of CO_2.

The changes of C_R and C_E of CO_2 were first presumed to arise from the dielectric constant of the barrier. This effect would be similar to that discussed by Kogelschatz [4], who noted that the high dielectric constant of the dielectric barrier would enhance the average plasma power, i.e., the power density, which means more discharges are initiated per unit of time and per unit of electrode/barrier area.

In fact, once the dielectric barrier discharge occurs, many charged particles will strike on the surface of the dielectric barrier to increase the temperature up to about 130 ℃. Surely, the dielectric loss also contributes to the increase of temperature. Hence, we compare the dielectric constant of the ceramic materials at 130 ℃ and find that there are only marginal differences among them as is shown in Fig.3 and summarized in Table 1. From the CO_2 decomposition measurements given above, we obtain the increasing tendency for C_R and C_E of CO_2 with increasing glass content. This indicates that the dielectric constant of the barrier will not dominate the CO_2 decomposition owing to the small differences among the barriers. Consequently, it is believed that the dielectric constant of the dielectric barrier is not directly related to the changes of C_R and C_E of CO_2.

Alternatively, we will consider the possibility that the changes of C_R and C_E of CO_2 depend on the surface resistivity. In previous studies, a charge spreading model, supposing that charges on the dielectric surface show an

Table 1 Dielectric constant and discharge properties of the CST ceramics as a function of glass content

Glass content/wt%	Dielectric constant (130 ℃/100 kHz)	P/W	C_R/%	C_E/% ·W^{-1}
0.5	282	11.52	11.56	1.00
1.0	296	11.24	27.88	2.48
5.0	278	11.58	67.14	5.67

Ohmic behavior, has been reported [12]. According to the model, the radial field E_r due to a surface point charge Q_p is defined by

$$E_r(r,0,t)=\frac{Q_p r}{4\pi\varepsilon_0\varepsilon_e(r^2+\upsilon^2t^2)^{3/2}_{t\rangle 0}} \quad (7)$$

where, ε_e is the effective dielectric constant, and υ is constant velocity defined by

$$\upsilon=\frac{1}{2\rho_s\varepsilon_0\varepsilon_e} \quad (8)$$

where, ρ_s is the surface resistivity. When using a dielectric barrier with low ρ_s, the radical field between Q_p and r with time is decreased fast, which means the fast charge spreading. In the process of DBD, charges produced from the plasma reaction will accumulate on the dielectric barrier and then easily spread over the whole surface because of the low surface resistivity. These widely distributed charges would initiate more microdischarges and consequently contribute to the discharge uniformity [6]. In fact, each individual microdischarge can be regarded as a miniature plasma chemical reactor [4] and the uniform discharge can produce much more reactors to effectively decompose chemical substances, such as CO_2. However, the C_R and C_E of CO_2 are not increased with the decrease of surface resistivity as shown in Fig.2. These results suggest the observed changes of the C_R and C_E of CO_2 are not due to the charge spreading model.

The above two interpretations based on the effects of the surface resistivity and the dielectric constant of the dielectric barrier seem reasonable. Further, the poor dependence of microstructure on the glass content should not yield comparable differences during the discharge process.

There are some reports proposing the possible mechanisms about how electrons can be released from a dielectric barrier[13,14], for example, the ion-electron emission, the electron desorption and secondary electron emission due to impinging ions and metastables in dielectric barriers. The logical explanation lies in the fact that plentiful electrons could bring about much more collisions effectively with the CO_2 molecules. Fig.8 represents the schematic diagrams with the proposed mechanism for the obtained changes in C_R and C_E of CO_2.

The positive ions deposited on the thin oxide film could produce surface polarization and then form a high potential gradient, resulting in the emission of electrons through the surface [15], which is called the Malter effect. The Malter effect needs three conditions to be established: (a) an insulator on the cathode, (b) the rate of ion buildup must be higher than that of its removal from the insulating layer, and (c) some ignition mechanism[16], which are met in our experiments. A dielectric barrier attached to one electrode, as shown in Fig.8, is subjected to polarization during one semi-period when a high ac voltage is applied on the electrodes to cause DBD and the electrons move to the high voltage electrode, while the positive ions move to the low voltage electrode to deposit on the surface of dielectric barrier. The electric field E_1 generated by the high voltage and low voltage electrode and E_2 generated by the positive ions and the electrons owing to surface polarization have the identical direction so that the electric field near the surface of dielectric barrier could reach 10^6 V/m to pull out the electrons into the gap space to decompose CO_2. As is depicted in Fig.8, the higher the glass content, the greater the amount of electrons near the surface of the dielectric barrier will be. It would enhance the Malter effect to initiate much denser and stronger microdischarges to decompose CO_2. Therefore, both the C_R and C_E of CO_2 increase with the increase of the glass content.

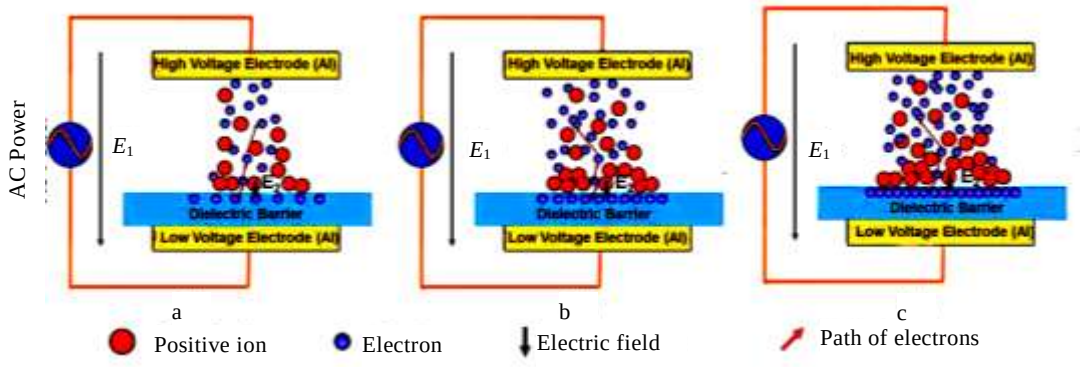

Fig.8 Schematic diagrams of Malter effect for the CST ceramics with BBS glass content of 0.5 wt% (a), 1.0 wt% (b), and 5.0 wt% (c)

3 Conclusions

1) The glass added $Ca_{0.8}Sr_{0.2}TiO_3$ ceramics are successfully prepared and utilized as the dielectric barriers in the decomposition of carbon dioxide.

2) Both the conversion rate and conversion efficiency increase with the increase of glass content. The Malter effect has important influence on the changes of conversion rate and conversion efficiency of carbon dioxide.

3) The high glass content could result in the increase of the amount of electrons near the surface of the dielectric barrier. Thus it would enhance the Malter effect to initiate much denser and stronger microdischarges to decompose CO_2.

References

1 Cui Naiyi, Brown Norman M D. *Applied Surface Science*[J], 2002, 189(1-2): 31

2 Chang Moo Been, Balbach J H, Rood M J *et al*. *Journal of Applied Physics*[J], 1991, 69(8): 4409

3 Eliasson Baldur, Hirth M, Kogelschatz Ulrich. *Journal of Physics D: Applied Physics*[J], 1987, 20: 1421

4 Kogelschatz Ulrich. *Plasma Chemistry and Plasma Processing*[J], 2003, 23(1): 1

5 Eliasson Baldur, Kogelschatz Ulrich. *IEEE Transactions on Plasma Science*[J], 1991, 19(2): 309

6 Choi Jai Hyuk, Lee Tae Il, Han Inho *et al*. *Applied Physics Letters*[J], 2006, 89(8): 081501

7 Li Ming, Li Chengrong, Zhan Huamao *et al*. *Applied Physics Letters*[J], 2008, 92(3): 031503

8 Li Ruixing, Tang Qing, Yin Shu *et al*. *Fuel Processing Technology*[J], 2006, 87(7): 617

9 Kraus Martin, Eliasson Baldur, Kogelschatz Ulrich *et al*. *Physical Chemistry Chemical Physics*[J], 2000, 3(3): 294

10 Wang Shuang, Zhang Yong, Liu Xiaolin *et al*. *Plasma Chemistry and Plasma Processing*[J], 2012, 32(5): 979

11 Massines Françoise, Gherardi Nicolas, Naudé Nicolas *et al*. *European Physical Journal Applied Physics*[J], 2009, 47(2): 22 805

12 Somerville I, Vidaud Patrick H. *Proceedings of the Royal Society of London: Series A*[J], 1985, 399(1817): 277

13 Golubovskii Yu B, Maiorovl V A, Behnke Jürgen F *et al*. *Journal of Physics D: Applied Physics*[J], 2002, 35(8): 751

14 Brandenburg Ronny, Maiorov V A, Golubovskii Yu B *et al*. *Journal of Physics D: Applied Physics*[J], 2005, 38(13): 2187

15 Louis Malter. *Physical Review*[J], 1936, 50(1): 48

16 Va'vra Jerry. *Nuclear Instruments and Methods in Physical Research Section A*[J], 2003, 515(1-2): 1

玻璃掺杂量对 $Ca_{0.8}Sr_{0.2}TiO_3$ 陶瓷介质阻挡层等离子体放电分解 CO_2 的影响

宋晓贞，张 勇，曲富洋，汪向荣

(清华大学 精细陶瓷北京市重点实验室，新型陶瓷与精细工艺国家重点实验室，北京 100084)

摘 要：通过液相烧结法成功制备出不同玻璃掺杂量的$Ca_{0.8}Sr_{0.2}TiO_3$陶瓷材料，并将该陶瓷材料作为介质阻挡层在圆柱型放电反应器中分解二氧化碳。研究结果发现，随玻璃掺杂量的增加，$Ca_{0.8}Sr_{0.2}TiO_3$陶瓷的表面电阻增大，但在所研究的温度范围内，$Ca_{0.8}Sr_{0.2}TiO_3$的介电常数并没有随玻璃掺杂量的变化而显著变化。扫描电镜结果表明，晶粒尺度和颗粒间玻璃相厚度随玻璃掺杂量增加而增大。另外，二氧化碳的转化率和转化效率随陶瓷中玻璃量的增加而提高。进一步采用Malter效应模拟放电和介电特性，根据该模型，可以解释转化特性与陶瓷样品中玻璃含量之间的关系。

关键词：介质阻挡放电；转化率；转化效率；二氧化碳

作者简介：宋晓贞，女，1986 年生，硕士，清华大学核能与新能源技术研究院，北京 100084，电话：010-80194055，E-mail: xzsongxz@126.com